Diode-pumped passively mode-locked 1.3-μm Nd:YVO_4 and Nd:YLF lasers by use of semiconductor saturable absorbers

R. Fluck, G. Zhang, and U. Keller

Ultrafast Laser Physics, Institute of Quantum Electronics, Swiss Federal Institute of Technology, ETH Hönggerberg-HPT, CH-8093 Zürich, Switzerland

K. J. Weingarten

Time-Bandwidth Products, ETH Hönggerberg-HPT, CH-8093 Zürich, Switzerland

M. Moser

Paul Scherrer Institute, CH-8048 Zürich, Switzerland

Received March 21, 1996

We report on self-starting passively mode-locked diode-pumped 1.3-μm lasers obtained by use of semiconductor saturable absorbers. We achieved pulses as short as 4.6 ps in Nd:YVO_4 and 5.7 ps in Nd:YLF with average output powers of 50 and 130 mW, respectively. © 1996 Optical Society of America

The development of a simple, compact, diode-pumped, mode-locked, solid-state laser at 1.3 μm is of wide interest. Applications of high-repetition-rate, ultrashort, high-power pulsed lasers are found in fiber-optic applications (telecommunications), fiber sensing, or ranging. Mode locking at 1.3 μm in Nd:YLF has been previously achieved both actively[1] and passively in a coupled-cavity (additive-pulse mode-locked) system.[2] Nd:YVO_4 was recently mode locked at 1 μm (Ref. 3) but has not been mode locked at 1.3 μm, to our knowledge.

In this Letter we demonstrate self-starting passively mode-locked Nd:YLF at 1314 and 1321 nm and Nd:YVO_4 at 1342 nm, using only an intracavity semiconductor saturable absorber. This permits a simple cavity design without an additional external cavity or drive and stabilization electronics. Pulse durations as short as 4.6 and 5.7 ps were achieved with Nd:YVO_4 and with Nd:YLF, respectively. Passive mode locking was achieved with either a high- or a low-finesse antiresonant Fabry–Perot saturable absorber (AFPSA) design.[4,5] This is our first demonstration of an AFPSA at 1.3 μm.

There are two key points to be considered for a 1.3-μm laser mode locked with a semiconductor saturable absorber. The first is the choice of the laser material in terms of gain cross section and upper-state lifetime, factors that determine the attainment of high gain and low pump threshold. The second consideration is the design and growth of the semiconductor saturable absorber, which are important for pure cw passive mode locking.

For most materials the gain cross section of the 1.3-μm transition is much smaller than the gain cross section of the 1-μm transition. Normally we wish to maximize the product of gain cross section and upper-state lifetime to achieve high small-signal gain and low pump threshold. But for passive mode locking a large gain cross section and a small upper-state lifetime are preferred to prevent Q switching.[6,7] We considered the Nd-doped laser crystals YLF and YVO_4. Nd:YVO_4 has a large gain cross section ($\approx 6 \times 10^{-19}$ cm^2), comparable with that of YAG at 1 μm, and a relatively small upper-state lifetime (100 μs).[8] Therefore it should be easier to passively mode lock. Additionally, its large absorption coefficient at 808 nm is attractive for diode pumping and further increases the small-signal gain when end pumped. Nd:YLF has a smaller gain cross section and a higher upper-state lifetime (450 μs) than Nd:YVO_4. Nevertheless, we have chosen to investigate Nd:YLF because of its better thermal properties and its wavelength, which better matches the transmission window of silica optical fiber.

We passively mode locked our lasers with an AFPSA, which consists of an intracavity saturable absorber lying between a highly reflecting Bragg bottom mirror and a top reflector. The nonlinearity is due to absorption bleaching of the semiconductor. Because we still want to benefit from the good quality of AlAs/GaAs Bragg mirrors, we need to grow the 1.3-μm saturable absorber layer upon a GaAs substrate. To achieve saturable absorption at 1.3 μm, the In concentration in the InGaAs absorber material must be increased to approximately 40%, which results in a significant lattice mismatch to the GaAs substrate. This lattice mismatch reduces the surface quality, resulting in higher insertion losses. The absorber material is grown by molecular-beam epitaxy at low temperature. There are two motivations for low-temperature growth. First, it partially relieves the lattice mismatch, which improves the optical quality of the absorber layer. Second, the lifetime of the absorber decreases into the picosecond regime, permitting the device to act as a fast saturable absorber to mode lock the laser.

In the experiments we used either a high-finesse [Fig. 1(a)] or low-finesse [Fig. 1(b)] AFPSA design, both of which have been well described by previous

0146-9592/96/171378-03$10.00/0

studies.[4,5] In our specific low-finesse design the spacer layer is one half of a standing wave, and the saturable absorber is positioned near the peak of the wave for maximum modulation depth. The half-wave spacer layer permits the saturable absorber to be easily positioned at the peak of the standing wave for maximum modulation depth. This design is similar to the saturable Bragg reflector design,[9] which simply uses a quarter-wave spacer layer and an embedded absorber. Note that both devices are intermediate designs between the previously reported high-finesse AFPSA (Ref. 4) and the antireflection-coated thin saturable absorber.[11] It is also worth noting that the Bragg reflector is not fundamentally necessary for these devices and is often a limitation for very short pulse widths; for example, a metal-mirror saturable device has produced 10-fs pulse widths.[11]

We measured the impulse response (Fig. 2), saturation fluence, insertion loss, and maximum modulation depth of the high- and low-finesse AFPSA's, using 150-fs-long pulses at 1.32 μm.[12] For picosecond pulses we would expect a slightly lower modulation depth but no change in the carrier lifetime and no significant change in the saturation fluence. For the high-finesse device we measured a lifetime of 9.5 ps, a maximum modulation depth of 0.2%, and a saturation fluence of 30 mJ/cm^2, whereas for the low-finesse device we measured a lifetime of 4 ps, a maximal modulation depth of $\approx$2%, and a saturation fluence of 0.4 mJ/cm^2. The maximum modulation depth is obtained well above the saturation fluence (i.e., typically greater than three times the saturation fluence[12]) and is approximately ten times larger for the low-finesse device. On the other hand, the nonsaturable losses of the high-finesse AFPSA are lower, i.e., only $\approx$0.1%, compared with that of the low-finesse device ($\approx$4%), which leads to higher output power. However, the insertion loss of the low-finesse AFPSA was too high for the Nd:YLF laser to yield stable mode locking with the available pump power.

We used a standard end-pumped cavity with a flat/Brewster-cut laser crystal and a 50-cm radius-of-curvature mirror. The laser crystals were 4-mm-long 1.5%-doped Nd:YLF and 3.5-mm-long 2%-doped Nd:YVO_4. As pump sources we used two 1-W 100-μm stripe-width pump diodes, which we focused to a 150 μm $\times$ 40 μm radius inside the Nd:YLF and a 80 μm $\times$ 30 μm radius inside the Nd:YVO_4. To passively mode lock the laser we replaced a high reflector by an AFPSA and a curved mirror to focus onto it. By varying the curvature of this mirror we are able to adjust the laser beam spot size of the AFPSA and therefore control the available incident pulse energy density with respect to the saturation fluence of the device. The spot size on the high-finesse AFPSA was set to a radius of approximately 30 μm with a 7.5-cm curved mirror and to approximately 100 μm with a 30-cm curved mirror for the low-finesse AFPSA. The output coupler was a fold mirror, producing two output beams, and the output coupling was 1% total (0.5% per beam).

Nd:YLF has two lasing transition lines at 1.3 μm. We preferred the σ line at 1314 nm because it showed a higher peak value in the measured fluorescence spectrum. The cw laser spectrum of Nd:YLF was tunable over a 6-nm bandwidth by use of a 1-μm-thick étalon. We mode locked Nd:YLF with a high-finesse AFPSA, achieving pulse widths of 5.7 ps (Fig. 3) at a repetition rate of 98 MHz. The average output power was 130 mW (one beam) at an absorbing pump power of 1.1 W. The lasing threshold was at 46 mW, and the optical slope efficiency was 30% cw. The peak power was 230 W, and the pulse energy density on the absorber was 9.3 mJ/cm^2, approximately three times less than the saturation fluence, resulting in only an $\approx$0.07% reflection modulation of the high-finesse AFPSA. The time–bandwidth product was 0.8 and thus was not transform limited, as expected from an end-pumped laser.[13]

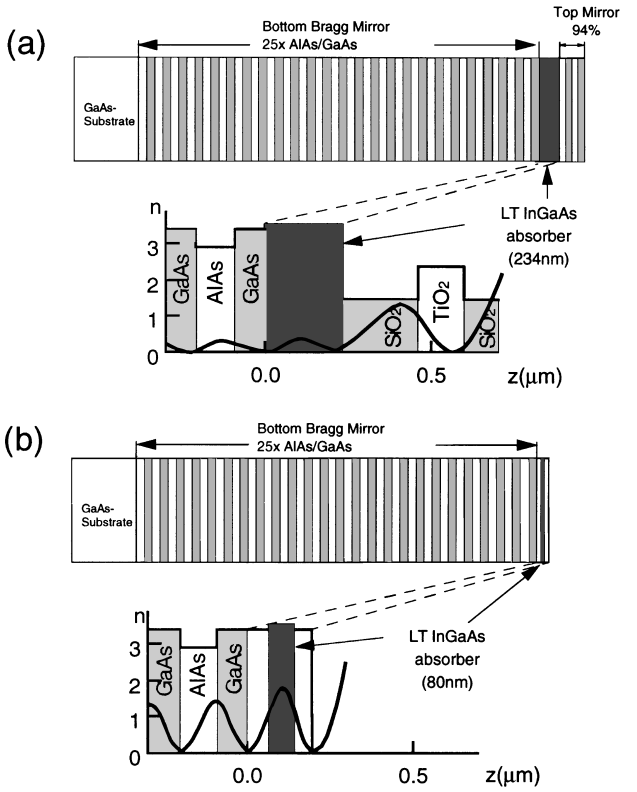

Fig. 1. Schematic structure and refractive-index profile with the standing-wave intensity distribution of (a) the high-finesse and (b) the low-finesse AFPSA.

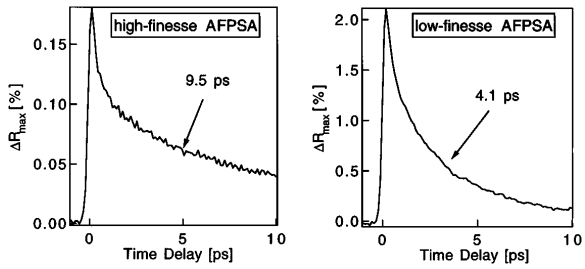

Fig. 2. Lifetime measurements with 150-fs pulses at a wavelength of $\approx$1.3 μm and a pulse energy density of approximately the saturation fluence for the high- and low-finesse AFPSA's. The maximum modulation depth of the low-finesse AFPSA is approximately ten times higher than that of the high-finesse device.

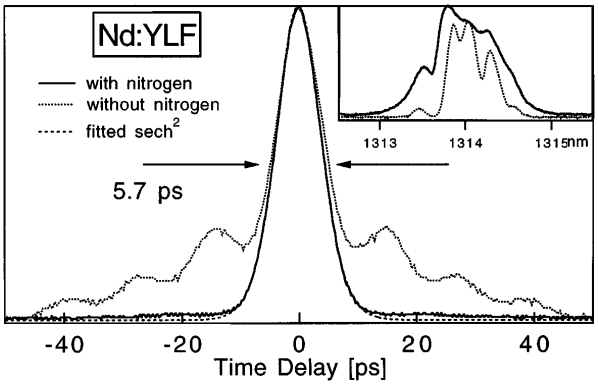

Fig. 3. Autocorrelation trace and spectrum of Nd:YLF when a high-finesse low-insertion-loss AFPSA is used, with and without nitrogen purging.

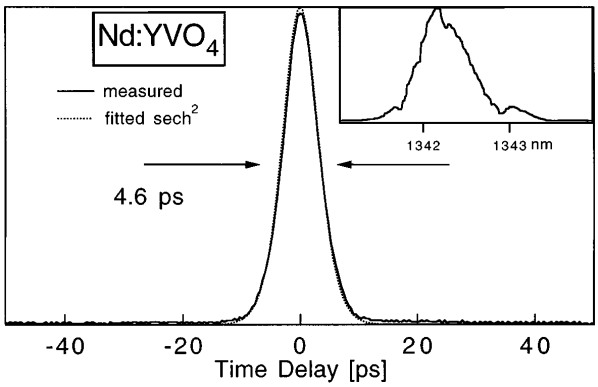

Fig. 4. Autocorrelation trace and spectrum of $Nd:YVO_4$ when a low-finesse AFPSA is used.

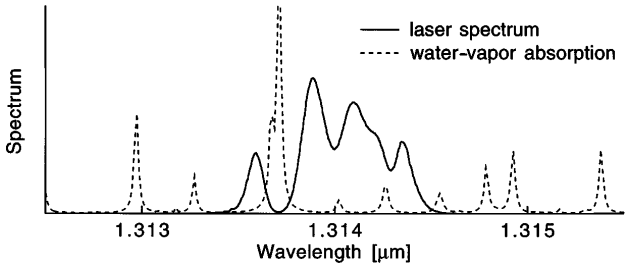

Fig. 5. Laser spectrum of Nd:YLF overlapped with the calculated water-vapor absorption lines.

With $Nd:YVO_4$ and the low-finesse AFPSA we achieved 4.6-ps pulses (Fig. 4) at a repetition rate of 93 MHz and a corresponding peak power of 120 W. The average output power was 50 mW (one beam) at an absorbed pump power of 1.2 W. The pulse energy density of the absorber was 340 $\mu J/cm^2$, slightly below the saturation fluence, resulting in an $\approx 0.6\%$ reflection modulation of the low-finesse AFPSA. The time–bandwidth product was 0.5, the lasing threshold was at 43 mW, and the optical slope efficiency was 21% cw.

Typically, shorter pulses can be achieved with the low-finesse AFPSA because of the higher modulation depth. But we could not achieve cw mode locking with Nd:YLF by using the low-finesse AFPSA because of the higher loss of this device and the small gain cross section of the laser material. By use of a high-finesse AFPSA with either Nd:YLF or $Nd:YVO_4$, the spectrum and autocorrelation were modulated. The holes in the measured lasing spectrum (Fig. 5) correspond to the water-vapor absorption lines. Our experimental results indicate that the modulation of the high-finesse AFPSA was too small to overcome the extra absorption of the water vapor in air, which was strong enough to modulate the spectrum and lead to longer pulses with significant pedestals or wings (Fig. 3). Clean pulses were achieved only after we purged the laser cavity with dry nitrogen. In contrast, no nitrogen purging was required when we used the low-finesse AFPSA with the $Nd:YVO_4$ laser. This most likely is the result of the larger modulation depth of the low-finesse AFPSA and the higher gain cross section of the laser material, which overcomes the residual water absorption lines in the spectrum.

In conclusion, we have demonstrated self-starting passive mode-locking with $Nd:YVO_4$ and Nd:YLF at 1.3 μm, using a low- and a high-finesse AFPSA with a lattice-mismatched InGaAs absorber layer on a GaAs substrate. $Nd:YVO_4$ was easier to mode lock because of its larger gain cross section, short upper-state lifetime, and large pump absorption coefficient. Nd:YLF has a relatively large fluorescence bandwidth, better thermal characteristics, and offers wavelengths closer to standard fiber applications.

This study was supported by the Swiss National Science Foundation.

References

1. F. Zhou, G. P. A. Malcolm, and A. I. Ferguson, Opt. Lett. **16,** 1101 (1991).
2. D. A. Armstrong, A. Robertson, N. Langford, and A. I. Ferguson, in *Conference on Lasers and Electro-Optics*, Vol. 15 of 1995 OSA Technical Digest Series (Optical Society of America, Washington, D.C., 1995), p. 334.
3. J. D. Kafka, J. Opt. Soc. Am. B **12,** 2147 (1995).
4. U. Keller, D. A. B. Miller, G. D. Boyd, T. H. Chiu, J. F. Ferguson, and M. T. Asom, Opt. Lett. **17,** 505 (1992).
5. U. Keller, Appl. Phys. B **58,** 347 (1994).
6. H. A. Haus, IEEE J. Quantum Electron. **12,** 169 (1976).
7. F. X. Kärtner, L. R. Brovelli, D. Kopf, M. Kamp, I. Calasso, and U. Keller, Opt. Eng. **34,** 2024 (1995).
8. R. A. Fields, M. Birnbaum, and C. L. Fincher, Appl. Phys. Lett. **51,** 1885 (1987).
9. S. Tsuda, W. H. Knox, E. A. D. Souza, W. Y. Jan, and J. E. Cunningham, Opt. Lett. **20,** 1406 (1995).
10. L. R. Brovelli, I. D. Jung, D. Kopf, M. Kamp, M. Moser, F. X. Kärtner, and U. Keller, Electron. Lett. **31,** 287 (1995).
11. R. Fluck, I. D. Jung, G. Zhang, F. X. Kärtner, and U. Keller, Opt. Lett. **21,** 743 (1996).
12. L. R. Brovelli, U. Keller, and T. H. Chiu, J. Opt. Soc. Am. B **12,** 311 (1995).
13. F. X. Kärtner, B. Braun, and U. Keller, Appl. Phys. B **61,** 569 (1995).